Pharm Res (2016) 33:337–357
DOI 10.1007/s11095-015-1793-0

RESEARCH PAPER

Thermodynamic Changes Induced by Intermolecular Interaction Between Ibuprofen and Chitosan: Effect on Crystal Habit, Solubility and *In Vitro* Release Kinetics of Ibuprofen

Amos Olusegun Abioye [1] • Rachel Armitage [1] • Adeola Tawakalitu Kola-Mustapha [1,2]

Received: 24 June 2015 / Accepted: 14 September 2015 / Published online: 24 September 2015

ABSTRACT

Purpose The direct impact of intermolecular attraction between ibuprofen and chitosan on crystal behaviour, saturated solubility and dissolution efficiency of ibuprofen was investigated in order to expand the drug delivery strategy for ibuprofen.

Methods Amorphous nanoparticle complex (nanoplex) was prepared by controlled drug-polymer nanoassembly. Intermolecular attraction was confirmed with surface tension, conductivity measurements and FTIR spectroscopy. The nanoplex was characterized using DSC, TGA and SEM. The *in vitro* release kinetics and mechanism of drug release were evaluated using mathematical models.

Results The cmc of ibuprofen decreased significantly in the nanoplex (1.85 mM) compared with pure ibuprofen (177.62 mM) suggesting a remarkable affinity between the chitosan and ibuprofen. The disappearance of ibuprofen melting peak in the nanoplex and the broadened DSC endothermic peaks of the nanoplex indicate formation of eutectic amorphous product which corresponded to higher saturated solubility and dissolution velocity. Ibuprofen (aspect ratio 5.16±1.15) was converted into spherical nanoparticle complex with particle size of 14.96±1.162–143.17±17.5247 nm (36–345 folds reduction) dictated by chitosan concentration. Pure ibuprofen exhibited burst release while the nanoplexes showed both fast and extended release profiles. DE increased to a maximum (81.76±2.1031%) with chitosan concentrations at 3.28×10–3 g/dm3, beyond which retardation occurred steadily. Major mechanism of drug release from the nanoplex was by diffusion however anomalous transport and super case II transport did occur.

Conclusion Ibuprofen-chitosan nanoplex exhibited combined fast and extended release profile dictated by chitosan concentration. This study demonstrated the potential application of drug-polymer nanoconjugate design in multifunctional regulated drug delivery.

KEY WORDS Ibuprofen-chitosan nanoplex · Surface excess · Solubility parameters · Thermodynamic properties · Mechanism of drug release

ABBREVIATIONS

ANOVA	Analysis of variance
CE	Conjugation efficiency
CT	Chitosan
DE	Dissolution efficiency
DSC	Differential scanning calorimetry
FT-IR	Fourier transform infra-red spectroscopy
HSD	Honest significant difference
IB	Ibuprofen
MDR	Mean dissolution rate
MDT	Mean dissolution time
MWCO	Molecular weight cut off
PEC	Polyelectrolyte complex
SEM	Scanning electron microscopy
TGA	Thermal gravimetric analysis
VT	Variance of dissolution time

INTRODUCTION

Chitosan (CT) is a unique cationic biopolymer containing randomly distributed β-1,4-linked glucosamine and N-acetyl-D-glucosamine units (Scheme 1a). It is prepared by

✉ Amos Olusegun Abioye
aabioye@dmu.ac.uk

[1] Leicester School of Pharmacy, De Montfort University, The Gateway Leicester LE1 9BH, UK

[2] Department of Pharmaceutics and Industrial Pharmacy, Faculty of Pharmaceutical Sciences, University of Ilorin, Ilorin, Nigeria

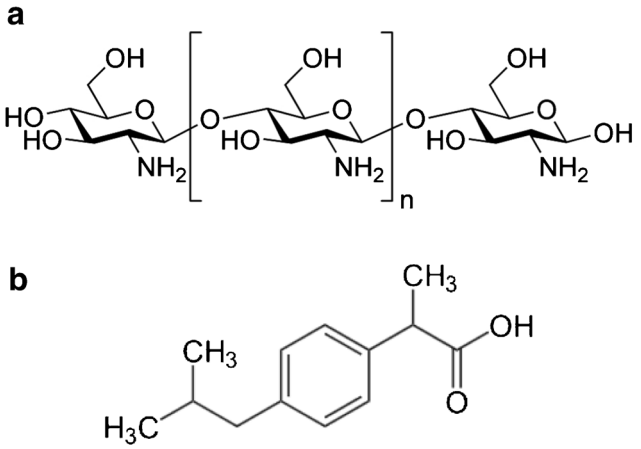

Scheme I Chemical structures of Chitosan (**a**); Ibuprofen (**b**).

N-deacetylation of chitin, a natural polysaccharide found in the exoskeleton of insects, shrimps, crabs and lobsters as well as fungi (1). CT has attracted increasing research attention due to its abundant availability, low production cost, nontoxicity, biocompatibility, biodegradability as well as inherent pharmacological properties(1, 2). It has wide applications in textile, food, agriculture, pharmaceuticals and biotechnology including nutrients, drug delivery and tissue engineering. Literature is replete with chitosan-based polyelectrolyte complexes (PEC) which are formed spontaneously by mixing oppositely charged polyelectrolytes in solution without any chemical crosslinker (1). Cationic polysaccharides containing non-polar region and ammonium groups have been reported to provide hydrogen bonding capacity and high affinity for oppositely charged molecules. On the other hand ionized ibuprofen species are surface active molecules capable of self-association in aqueous solutions (3) and able to adsorb onto polymers through hydrophobic and electrostatic bonds (conjugation) with their aromatic ring and hydrophilic carboxylic groups respectively (4–9) which may induce useful changes in the crystal habit as well as the controlled release process of the drug. It was envisioned that the high density positive charges of chitosan (due to the protonation of amino groups on its backbone at low pH) will interact with negatively charged ibuprofen (IB) species to form drug-polymer complex of submicron size with improved biopharmaceutical properties. Therefore this study investigates the direct effect of ibuprofen-chitosan (IB-CT) complexation on the crystal habit, physicochemical characteristics and the release mechanism of ibuprofen. CT was used in this study because of its abundant natural occurrence, ability to form polyelectrolyte complexes, biocompatibility, low toxicity, good mechanical properties and long resident times at the site of application(10). Biodegradable polyelectrolyte nanocarriers such as nanoparticles, nanocapsules, micellar systems, and nanoconjugates have been the focus of intensive research for the delivery of poorly soluble drugs because they provide great opportunities in the area of controlled drug release and site specific drug delivery due to their submicron size (11, 12).

Ibuprofen [(RS)-2-(4-(2-methylpropyl)phenyl)propanoic acid, Scheme 1b] is an effective non-steroidal anti-inflammatory drugs (NSAID) used for the management of pain, fever, symptoms of rheumatoid arthritis and osteoarthritis. However because of its needle-like (acicular) crystalline nature, viscoelastic and high cohesive characteristics, low solubility (49 μg/ml at 25°C) and short biological half-life (2 h), ibuprofen has been difficult to formulate and when administered orally, large and multiple doses are usually required, leading to wasted dosing and potentially serious side effects such as ulceration and bleeding (4, 5, 13). Therefore there is continuous research interest to enhance the biopharmaceutical properties and system specific parameters of ibuprofen. It is common knowledge that a successful drug delivery requires effectiveness and safety of therapy. In essence, the concentration of the drug should be high enough to ensure therapeutic effect however excessive doses should be avoided because this may result in potentially harmful side effects. In order to improve the biopharmaceutical properties of ibuprofen, amphiphilic drug-biocompatible polymer conjugates have been the focus of formulation research in the recent past (5, 6, 8, 14). Literature is replete with research reports on chitosan-based polyelectrolyte complexes with oppositely charged natural and synthetic polyelectrolytes however the general problem of aqueous association of poorly soluble amphiphilic drug and poorly water soluble polymers remain unresolved. To our knowledge, the direct effect of ibuprofen-chitosan (IB-CT) complexation on solubility parameters and mechanism of release of ibuprofen have not been reported in literature. It was hypothesized that the ionized ibuprofen species (amphiphilic molecule) will interact with cationic chitosan to produce IB-CT nanoparticle complex (*nanoplex*) with enhanced ibuprofen solubility and dissolution parameters. By understanding the mechanism of this interaction, it may be possible to design system-specific drug-polymer formulations that will overcome the poor biopharmaceutical characteristics of ibuprofen.

MATERIALS AND METHODS

Materials

Ibuprofen was purchased from Fagron UK (Newcastle upon Tyne, UK), low molecular weight chitosan (MW 22 kDa) was purchased from Sigma–Aldrich (Gillingham, Dorset, UK) and were used as supplied without further purification. All other chemicals used were of an analytical grade. Double distilled water was used throughout the study.

Methods

Preparation of IB-CT Nanoplex

The polymer-drug nanoparticle complex was prepared according to the previously described technique (6). Briefly, double strength molar concentrations of Chitosan (CT) ranging from 5.0×10^{-4} to 1.6×10^{-2} mM was prepared in 2–5 ml of 1% glacial acetic acid and made up to 25 ml with de-ionized water at room temperature (18°C) under continuous magnetic stirring (1000 rpm) in a jacketed vessel on a water bath (B Braun Certomat WR Shaker water bath, Germany). Double strength molar concentrations of ibuprofen (2.42, 4.85, 9.70 and 19.40 mM) were dissolved in 3–5 ml of sodium hydroxide (0.1 M) and made up to 25 ml with de-ionized water. Ibuprofen (IB) solution was added drop wise to the CT solution with continuous stirring for 24 h. The total volume of the *nanoplex* colloidal dispersion (50 ml) contains 1.21, 2.42, 4.85 and 9.70 mM of ibuprofen and 2.5×10^{-4} to 8.0×10^{-3} mM of CT respectively. The colloidal dispersion of each drug polymer molar ratio was transferred quantitatively into separate dialysis tube (MWCO 14,000 Da) and placed in 900 ml double distilled water in a USP XXI six stage paddle dissolution apparatus at 25°C and 50 rpm paddle rotation. The deionised water was changed three times after each dialysis cycle time of 3 h. At the end of the three cycles (9 h), all the water washings were pooled together and evaluated spectroscopically to determine the amount of un-conjugated ibuprofen at 264 nm. The colloidal dispersions of the nanocomplex were transferred into 50 ml centrifuge tubes and centrifuged at 5000 rpm for 1 h. The pellet was re-suspended in deionized water and the process repeated twice. Samples were dried at 40°C for 3 h and kept airtight amber glass bottles at ambient temperatures until ready for analysis. Five replicate (a total of six sets) of samples were prepared for each batch.

Characterization of IB-CT Nanoplex

Surface Tension. Surface tension of various concentrations of chitosan, ibuprofen and their *nanoplex* dispersions were determined separately at 20°C on torsion balance (dynamometer) using Du Noüy platinum ring of 4 cm diameter (White Elec. Inst, Co. Ltd). The maximum force required to detach (tear-off) the platinum ring from the surface of the liquid surface was determined and surface tension was calculated from Eq. 1 (15, 16). The surface tension measurements were an average of at least six determinations.

$$\gamma = \left[\frac{F}{4\pi R}\right] \times C \tag{1}$$

where F is the force required to detach the ring from the liquid surface, R is the radius of the ring and C is the correction factor depending on the density of the liquid, radius of the ring and the radius of the wire with which the ring was made.

Ibuprofen-Chitosan Complexation Efficiency. The amount of ibuprofen that forms the IB-CT *nanoplex* was calculated as the difference between the amounts of ibuprofen added and the amount of non-complexed ibuprofen in the dialysis washings after 9 h of dialysis process (Eq. 1). Five milliliters of the dialysis washings was passed through a 0.45 μm disposable Millipore membrane filter (Sartorius, Germany) and diluted to a suitable concentration with de-ionized water. The non-conjugated ibuprofen concentration was determined using UV – visible spectrophotometer (ThermoFischer Evolution 60 UV Spectrophotometer, UK) at 264 nm. All measurements were an average of six determinations.

$$\text{Complexation efficiency} = \frac{M_i - M_n}{M_i} \times 100\% \tag{2}$$

Where M_i is the initial amount of ibuprofen added and M_n is the amount of non-conjugated ibuprofen in the dialysis washings after 9 h.

Fourier Transforms Infrared Spectroscopy (FT-IR). The method described previously by Abioye *et al.* (6, 8) was adapted to investigate the structural changes in IB-CT *nanoplex* compared with the pure ibuprofen and raw chitosan. Briefly, about 10 mg of each sample was placed on the diamond surface plate of the Perkin-Elmer Precisely Spectrum One FTIR Spectrometer with Universal ATR Sampling Accessory (Perkin Elmer, USA). The air within the laboratory environment was used as blank. Sufficient pressure (100–120 units) was applied for close contact compression. The spectrum for each sample, including the controls, was recorded within the wave number range of 4000–400 cm^{-1} at an average of 16 scans and resolution of 4 cm^{-1}. All measurements were taken in replicate of six determinations.

Scanning Electron Microscopy (SEM). The shape and surface topography of pure ibuprofen crystals, chitosan and the *nanoplex* samples were determined by using Carl Zeiss SEM EVO High Definition 15 Scanning Electron Microscope (Carl Zeiss, Germany) operating at 15 kV. The samples were mounted on a metal stub with double-sided adhesive tape and gold-coated under vacuum in an argon atmosphere prior to observation. Particle size was determined using *SmatTiff* software and average of a minimum of 20 nanoparticle complex was determined within the microscopic view of each of the six replicate in each batch giving a total of 120 particles per batch.

Differential Scanning Calorimetry (DSC). As described previously (6, 8). Perkin Elmer Precisely Jade DSC machine with a Perkin Elmer Intracooler SP cooling Accessory and Pyris

Software (PerkinElmer Ltd., Beaconsfield, UK) was utilized to evaluate the thermal behaviour of the *nanoplex* compared with pure ibuprofen and raw chitosan. The temperature and heat flow of the instrument were calibrated using an indium and zinc standards. The sample sizes in the range of 5–8 mg were heated in hermetically sealed aluminium pans under nitrogen flow (40 ml/min) using a scanning rate of 20°C/min from −50 to 300°C. Empty aluminium pan was used as a reference. All measurements were an average of four determinations and expressed as mean ± S.D.

Thermal Gravimetry Analysis (TGA). The rate and extent of weight change of the *nanoplex* relative to temperature, was evaluated with Perkin Elmer Pyris 1 Thermogravimetric Analyser (PerkinElmer Ltd., Beaconsfield, UK) and compared with pure ibuprofen and raw chitosan. Standard references (Alumel and nickel) were used to calibrate the weight profile. Samples of known weight (3–5 mg) were analysed in crimped aluminium pans placed in crucible baskets at a scanning rate of 10°C/min between 25 and 500°C. All measurements were an average of four determinations and expressed as mean ± S.D.

Determination of Saturation Solubility of Ibuprofen Nanocomplex

Phase solubility study was performed according to the technique described by Connors (17). Excess amount of pure ibuprofen or IB-CT *nanoplex* (containing $0.82–26.21 \times 10^{-4}$ g/dm^3 chitosan) was placed in 50 ml centrifuge tubes with screw caps, containing 50 ml de-ionized water. The tubes were placed on a thermostatic mechanical shaker water bath (120 agitations / minute) for a total of 72 h at 18, 25 and 37°C respectively. The equilibrium time was established by quantifying the ibuprofen concentration until a constant value was obtained. Samples were taken every 2 for 8 h and subsequently every 24 h. At equilibrium, the supernatant solution was filtered through 0.45 μm Millipore membrane filter and diluted to a suitable concentration with the de-ionized water. The amount of ibuprofen dissolved was analysed using UV – Visible Spectrophotometer (Evolution 60S, Thermo Scientific, China) at 264 nm. Saturation solubility was determined at the point where there was no further increase in the amount of drug dissolved. All measurements were an average of six determinations.

In Vitro Release of Ibuprofen from the Binary Nanocomplex

The technique described previously by Abioye *et al.* (5, 6) by was adapted. Briefly, the Pharma Test Dissolution tester DT70 was set up to conform to USP XXI six stage dissolution apparatus II (paddle) method. Nine hundred milliliters of phosphate buffer (pH 7.4) was used as the dissolution medium, maintained at 37 ± 0.5°C throughout the study. The samples of pure ibuprofen powder and IB-CT *nanoplex* containing 100 mg of ibuprofen or its equivalent were weighed into small watch glass and placed at the bottom of the dissolution medium with the aid of a sample holder and stirred at 100 rpm using a rotating paddle. Five milliliters aliquot samples were withdrawn at pre-determined time intervals and 5 ml of fresh dissolution medium was replaced after each sampling to maintain sink condition. Each sample was filtered and diluted appropriately with the dissolution medium. The absorbance of the diluted solutions were measured at 264 nm using UV – Visible Spectrophotometer (Evolution 60S, Thermo Scientific, China) against the dissolution medium as the blank. Each measurement was an average of six determinations. Percentage drug release was calculated using the equation obtained from the calibration curve of ibuprofen secondary standard prepared under the same experimental conditions.

Quantitative Analysis of Dissolution Data. Time-point and pairwise model-independent analyses were used to characterize the release pattern of ibuprofen from the *nanoplex*. Model-independent approach produces a single value from the dissolution profile, providing direct comparison between different dissolution data which is suitable for dosage forms with different mechanisms (18–20). In the time-point approach, Mean Dissolution Times (*MDT*), Mean Dissolution Rate (*MDR*) and Dissolution Efficiency (*DE*) (area under the dissolution curve up to time *t*) were calculated according to Eqs. 3 to 5 respectively.

$$MDT = \frac{\sum_{i=1}^{n} t_i \Delta M_i}{\sum_{i=1}^{n} \Delta M_i} \tag{3}$$

where i is the sample number; t_i is the midpoint time period between t_{i-1} and t_i calculated as $(t_i + t_{i-1})/2$; n is the number of dissolution sample times and ΔM_i is additional amount of drug dissolved between t_i and t_{i-1}. Higher MDT values indicate lower drug releasing capacity of the conjugate crystanules and vice versa

$$MDR = \frac{\sum_{i=1}^{n} \Delta M_i / \Delta t}{n} \tag{4}$$

where n is the number of dissolution sample times; i is the sample number; Δt is the time at midpoint between t_{i-1} and t_i calculated as $(t_i + t_{i-1})//2$ and ΔM_i is additional amount of drug dissolved between t_i and t_{i-1}. Higher MDR values indicate higher drug releasing capacity of the *nanopplex* and vice versa.

$$DE(\%) = \frac{\int_0^t Y \times dt}{Y_{100} \times t} \times 100 \tag{5}$$

where Y is the percentage of ibuprofen dissolved at time t

In the pairwise approach, the variance of dissolution times (VT) as well as difference factor (f_1) were used to estimate the relative percent error (dissimilarity) between the dissolution data of treated and untreated ibuprofen using Eqs. 6 and 7 respectively (21).

$$VT = \frac{\sum_{i=1}^{n}(t_i - MDT)^2 \Delta M_i}{\sum_{i=1}^{n} \Delta M_i} \quad (6)$$

$$f_1 = \frac{\sum_{i=1}^{n} |R_t - T_t|}{\sum_{i=1}^{n} R_t} \quad (7)$$

where R_t and T_t are the percent drug dissolved from the pure ibuprofen as reference and the IB-CT *nanoplex* (test) at each sample point respectively. f_1 gives the approximate value of percent error between two dissolution profiles. The percent error is zero when the test and reference profiles are identical and increases proportionally with dissimilarity between the two profiles (21).

The similarity factor (f_2) was also determined as outlined in the SUPAC and IVIVC guidelines (22, 23) using the mean percentage ibuprofen release values in the *nanoplex* (test) compared with pure ibuprofen (reference) to estimate the similarity between them. It is the logarithmic reciprocal square root transformation of the sum of squared error of the differences between the dissolution profiles of the reference and test products across the dissolution time (Eq. 8).

$$f_2 = 50 \ log\left\{\left[1 + \frac{1}{n}\sum_{i=1}^{n} w_t (R_t - T_t)^2\right]^{-0.5} \times 100\right\} \quad (8)$$

Where n is the number of sample points, w_t is an optional weight factor, R_t is the reference assay at time point t and T_t is the test assay at time point t.

An f_2 value of 50 to 100 was defined as similarity between two dissolution profiles. The closer the $f_2$value to 100, the more identical are the release profiles while decrease in f_2 value suggests dissimilarity between the dissolution profiles (19, 21) The fit factors (f_1 and f_2) were validated by calculating the values for individual dissolution data of each batch which produced no statistically significant difference ($p > 0.05$; $n = 6$) between the mean dissolution values.

Mechanism of Ibuprofen Release from IB-CT Nanoplex

The mechanism of release of ibuprofen from the *nanoplex* was determined by fitting the kinetics of drug released into mathematical models including zero order kinetics; first order kinetics; Higuchi; Hixson-Crowell and Korsmeyer-Peppas (24). Dissolution profiles of less than 60% release were selected for the model fitness analysis. The degree of fitness into the mathematical models was used to evaluate the mechanism of drug release

Statistical Analysis

One way analysis of variance (ANOVA) was used to test differences in the percent of ibuprofen dissolved at each time point separately while multiple variate ANOVA was used to compare the dissolution kinetics of *nanoplex* at different concentrations of chitosan and time points. Tukey's HSD post-hoc test of the IB-CT *nanoplex* against the reference IB was also performed where Null hypothesis was rejected (25, 26). SPSS 8.0 for Windows (SPSS, Chicago, IL) was employed for the ANOVA based technique while Student *t*-test was used to determine any significant differences between test samples and the control. Differences were considered statistically significant when $p < 0.05$.

RESULTS AND DISCUSSION

Optimization of Ibuprofen-Chitosan Nanoparticle Complex

Ibuprofen was dissolved in 0.1 M NaOH, above its pKa (pH 4.5–5.3) to produce a highly soluble carboxylate species (27). In contrast, chitosan was dissolved in 1%v/v glacial acetic acid, below its pKa (pH 5.5–6.5), to produce a reactive functional group (protonated amine D-glucosamine monomeric unit). The interaction between the negative carboxylate ion of ibuprofen and the protonated amine groups in chitosan was optimized by controlling the formulation variables such as pH, ionic strength, ibuprofen concentration, chitosan concentration, drug-polymer ratio, mixing time, mixing speed, temperature and order of drug-polymer addition (results not presented). Evidence of interaction between ibuprofen and chitosan was investigated by determining the respective surface tension in aqueous dispersion of various concentrations of ibuprofen in chitosan solution and vice versa. Figure 1a shows decreasing surface tension to minimum values with increasing concentrations of pure ibuprofen suggesting surface activity. Pure ibuprofen exhibited two break points, calculated from the intersection points of the two linear regression lines before and after each break point, [0.0956 ± 0.0071 mg/ml (0.46 ± 0.0344 mM); $r^2 = 0.9935$ and 36.64 ± 1.4516 mg/ml (177.62 ± 4.088 mM); $r^2 = 0.9932$] corresponding to the *critical association concentration (cac)* and *critical micelle concentration (cmc)* respectively. The *cac* observed at low concentrations of ibuprofen may be explained by the ability of the amphiphilic ibuprofen molecules to form self-assemblies through the polar carboxylic acid group above certain concentration threshold in the aqueous medium (28). Romero *et al.*, (29) have reported that a single crystal unit of ibuprofen contains four ibuprofen

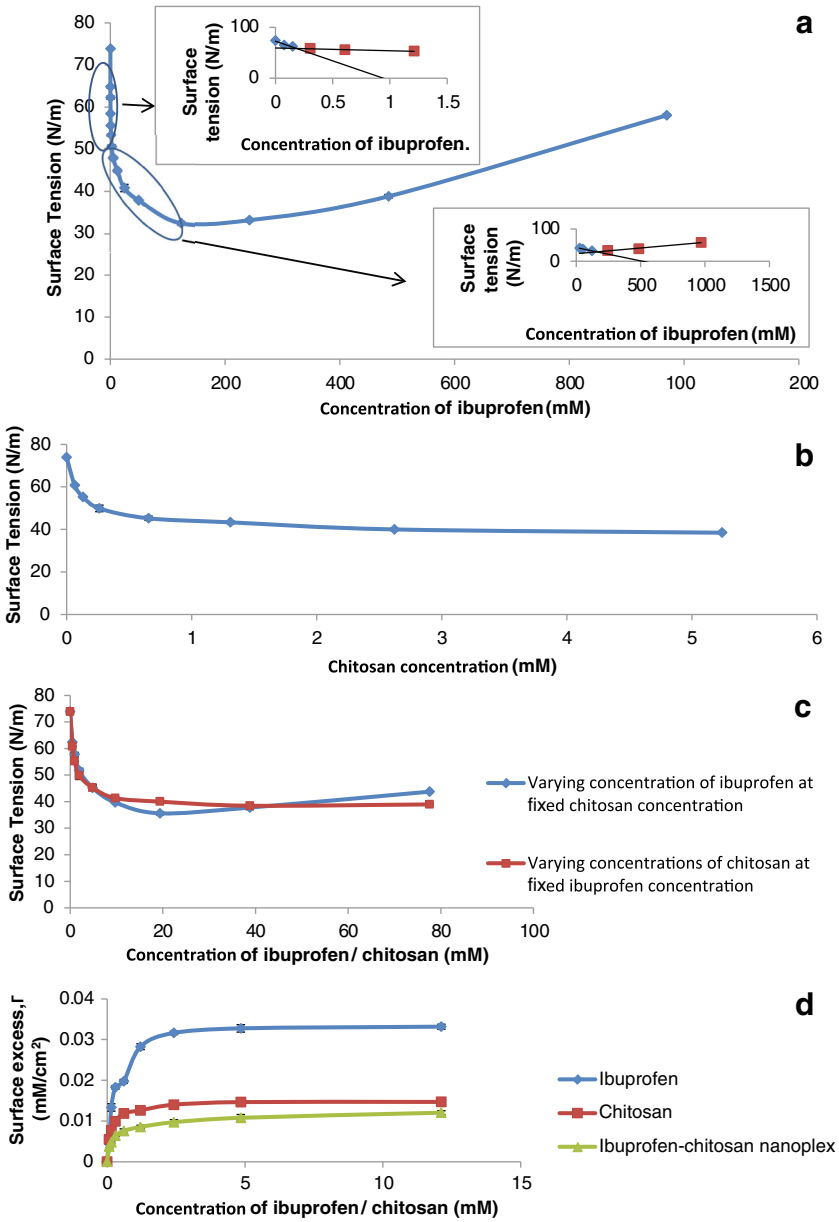

Fig. 1 The plot of Surface tension *versus* concentration of (**a**) pure ibuprofen; (**b**) chitosan alone (**c**) IB-CT *nanoplex* and (**d**) their respective surface excess.

molecules attached to each other by two hydrogen bonds from the polar carboxylic acid groups. The two free carboxylic acid groups are therefore available for binding to neighbouring units forming a mutually bonded hydrophilic unit in hydrophobic crystal structure. The observed *cmc* for pure ibuprofen (177.62±4.088 mM) was slightly lower than the reported value in literature (180 mM) by Ridell *et al.*, (30) probably due to differences in experimental conditions or variation in the purity of ibuprofen sample. The authors used ibuprofen sodium salt while acidic ibuprofen was used in this study. The ability of ibuprofen to form micelle-like aggregates above *cmc* similar to typical surfactants has also been reported in literature (31). Pure chitosan exhibited one break point (Fig. 1b) at 0.1471 mg/ml (0.0964 mM) indicating its *critical micelle concentration (cmc)*, which also suggests surface activity.

In the presence of chitosan ibuprofen exhibited two minima break points at 0.3821 mg/ml (1.8525 mM) and 2.4814 mg/ml (12.0292 mM) respectively (Fig. 1c). The first break point was ascribed to the *critical association concentration (cac)* where the interaction between chitosan and ibuprofen starts while the second break point, *cmc*, was attributed to the concentration of ibuprofen at which the ibuprofen-chitosan micelle-like aggregate occurred suggesting multiple complexation phenomena. This is similar to our previous findings with ibuprofen-cationic dextran conjugates (6). The significantly reduced *cmc* of the IB-CT *nanoplex* (1.85 mM) compared to the pure ibuprofen (177.62 mM) suggests a remarkable affinity between the cationic chitosan and ibuprofen ($p<0.05$; $n=6$), providing evidence for the drug-polymer (IB-CT) self-assembly without any chemical crosslinking agent. The interfacial concentration

of ibuprofen in excess of that in the bulk of the *nanoplex* dispersion (surface excess, Γ) was calculated from the Gibb's equation:

$$\Gamma = -\frac{C}{RT}\left[\frac{d\gamma}{dC}\right] \quad (9)$$

where Γ is the surface concentration of IB in excess of that in the bulk of the liquid (mM/cm^2); C is the concentration of IB in liquid bulk (mM); R is the Gas constant (8314 J mM^{-1}K^{-1}); T is the absolute temperature (K); dγ is the change in surface tension and dC is the change in bulk concentration.

The surface excess of ibuprofen, chitosan and IB-CT *nanoplex* are positive, increasing gradually to maximum values (Fig. 1d) indicating greater concentration of IB and CT in a unit cross-section of the interface than in the bulk region which confirms their surface activity and potential for intermolecular interaction. The maximum surface excess of IB decreased significantly ($p<0.05$; $n=6$) in the *nanoplex* (after IB-CT complexation) in the order 3.32 10^{-2}, 1.47×10^{-2} and 1.20×10^{-2} mM/cm^2 for IB, CT and IB-CT *nanoplex* respectively suggesting that the drug-polymer adsorption reduced the surface activity of IB. At maximum Γ a dynamic equilibrium was attained where surface tension could not be reduced any further corresponding to the critical micelle concentration and polymer saturation point for IB and *nanoplex* respectively. In the same vein, a comparative study with conductivity measurements showed reduction of the *cmc* of ibuprofen from 168.45 to 1.8908 mM ($r^2=0.9993$; results not presented) which correlates well with the surface tension results confirming strong molecular affinity and amplified molecular interaction between IB and CT.

SEM Photomicrographs of Ibuprofen-Chitosan Self-Assembly

Figure 2 shows the morphological characteristics of pure ibuprofen, chitosan and their nanoparticle complexes under Scanning Electron Microscope (SEM). Pure ibuprofen (Fig. 2a) exhibits distinct rod-like shape with smooth regular surface and average size $453.88\pm29.8469\times97.12\pm5.4267$ μm (aspect ratio 5.16 ± 1.15) as reported previously (4). Chitosan showed rough surface and irregular polyhedral shapes. The IB-CT *nanoplex* exhibited spherical nanostructures with remarkable decrease in particle size ($p<0.05$; $n=120$) as concentration of chitosan increased (Fig. 3a–c), losing the rod-like crystalline structure of pure ibuprofen. This may be explained by the disruption of the crystal lattice of ibuprofen due to the IB-CT intermolecular interaction. The spontaneous electrostatic nano-assembly of the oppositely charged molecules may have prevented ibuprofen from reverting back into the ordered crystalline form. As chitosan concentration increased, particle size of IB-CT nanoplex decreased to sizes within nanometre range (14.96 ± 1.1621–143.17 ± 17.5247 nm) (Figs. 2c–h and 3). The bioadhesive characteristics of chitosan was evident as the *nanoplex* associated to form loose aggregates (Fig. 3b and c) whose size increased from 223.58 ± 10.5762 to 701.33 ± 33.1684 nm with increasing concentration of chitosan (Fig. 3a). The individual nanoparticle within the nanoassembly maintained well defined spherical identity suggesting a reversible physical aggregation rather than particle growth. It was concluded that amphiphilic ibuprofen molecule interacted with chitosan to form micelle-like nanoassembly above critical aggregation concentration (*cac*) similar to the reports of Khan *et al.* (14).

Conjugation Efficiency

The conjugation efficiency (CE) of binary ibuprofen-chitosan nanoparticle complex is presented in Table IV. The lowest detectable CE (10.57 ± 0.5070%) was observed at low concentrations of chitosan (0.82×10^{-4} g/dm^3). CE increased steadily with chitosan concentration to a maximum of 98.75 ± 5.6619% at 26.24×10^{-3} g/dm^3 chitosan. This trend corresponds to increase in polymer saturation points (*psp*) of chitosan as its concentration increased. This is consistent with the decrease in particle size of IB-CT *nanoplex* with chitosan concentration as shown in the SEM data, similar to our previous report on ternary nanogel (8). Literature is replete with the CE of ibuprofen in several polymers including 9% in Eudragit polymeric nanoparticles (32); 10% in lipid nanoparticles e.g., smectic cholesterol ester nanoparticles (33); 30% in polymer-coated SiO_2 particles (34) and 37–71% in a chemically synthesized ibuprofen-dextran (dextran ester) conjugates (35). High value of CE obtained in this study was ascribed to the remarkable reduction in particle size and strong affinity as well as intermolecular interaction between ibuprofen and chitosan. Increasing CE with chitosan concentration could also be explained by increase in polymer saturation point (*psp*) and hydrophobic groups available for interaction with ibuprofen molecules resulting in higher CE.

Characterization of IB-CT Nanoplex

FT-IR Spectra Analysis

The FTIR spectra characteristics of pure ibuprofen, chitosan and their *nanoplexes* are shown in Fig. 4. The pure ibuprofen exhibited broad peaks between 3089 and 2631 cm^{-1} corresponding to OH group from carboxylic acid. These frequencies are lower than the non-bonded primary alcohol OH stretch (3645–3630 cm^{-1}) probably due to the impact of

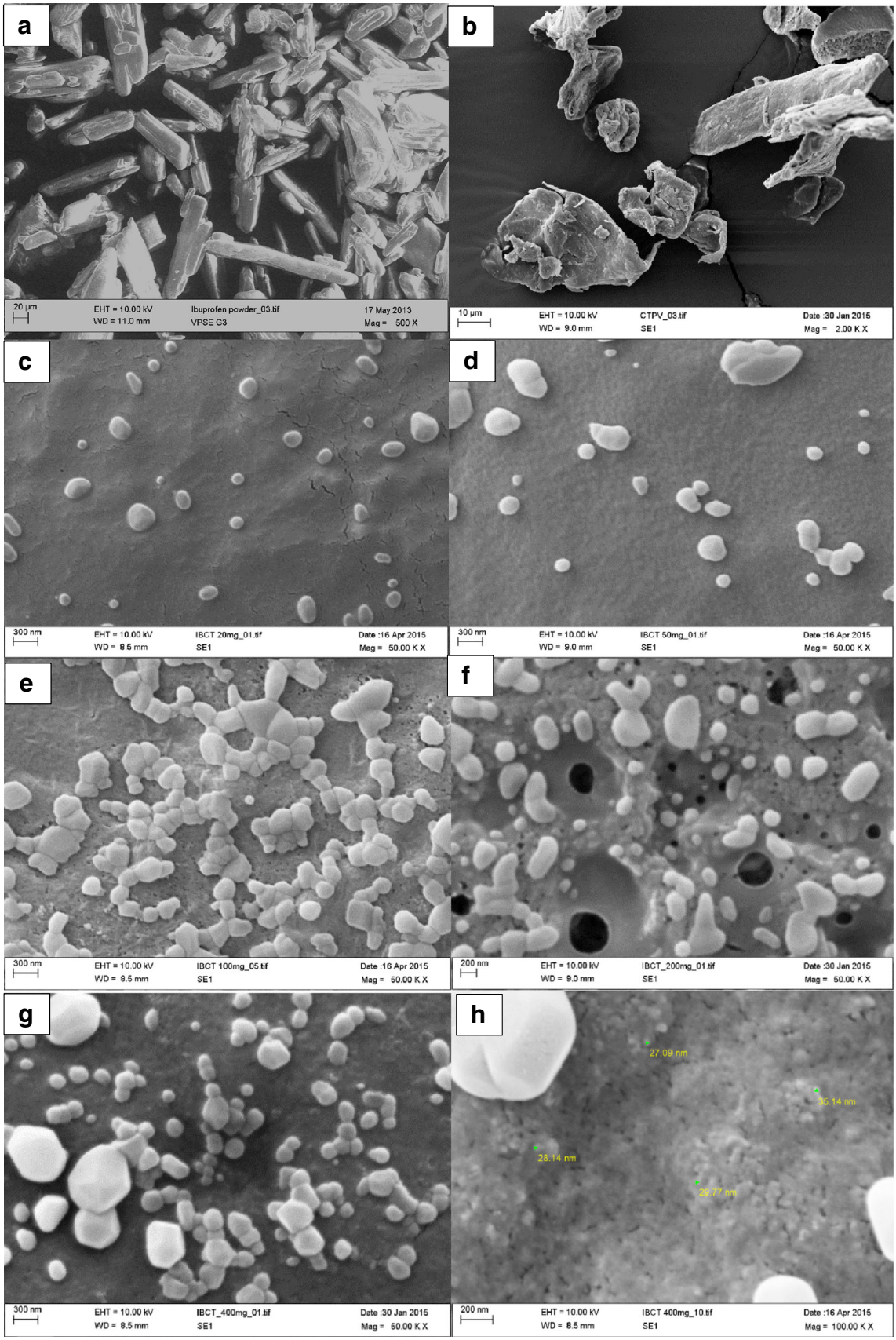
a
20 µm
EHT = 10.00 kV
WD = 11.0 mm
Ibuprofen powder_03.tif
VPSE G3
17 May 2013
Mag = 500 X
b
10 µm
EHT = 10.00 kV
WD = 9.0 mm
CTPV_03.tif
SE1
Date :30 Jan 2015
Mag = 2.00 K X
c
300 nm
EHT = 10.00 kV
WD = 8.5 mm
IBCT 20mg_01.tif
SE1
Date :16 Apr 2015
Mag = 50.00 K X
d
300 nm
EHT = 10.00 kV
WD = 9.0 mm
IBCT 50mg_01.tif
SE1
Date :16 Apr 2015
Mag = 50.00 K X
e
300 nm
EHT = 10.00 kV
WD = 8.5 mm
IBCT 100mg_05.tif
SE1
Date :16 Apr 2015
Mag = 50.00 K X
f
200 nm
EHT = 10.00 kV
WD = 9.0 mm
IBCT_200mg_01.tif
SE1
Date :30 Jan 2015
Mag = 50.00 K X
g
300 nm
EHT = 10.00 kV
WD = 8.5 mm
IBCT_400mg_01.tif
SE1
Date :30 Jan 2015
Mag = 50.00 K X
h
27.09 nm
35.14 nm
28.14 nm
29.77 nm
200 nm
EHT = 10.00 kV
WD = 8.5 mm
IBCT 400mg_10.tif
SE1
Date :16 Apr 2015
Mag = 100.00 K X

◀ **Fig. 2** Scanning electron micrographs showing the surface characteristics of (**a**) pure ibuprofen crystals; (**b**) pure Chitosan; and IB-CT *nanoplex* containing (**c**) 0.82; (**d**) 1.64 (**e**) 3.28; (**f**) 6.56; (**g**) 13.12 and (**h**) 26.24×10^{-3} g/dm^3 CT respectively.

hydrogen bonding which produces significant band broadening and lower mean absorption frequency (36). It has been reported that carboxylic acids exhibit extremely strong hydrogen bonding resulting into a stable dimeric structure with lower frequency. The strong, sharp carbonyl peak (C=O); aromatic ring vibration (C=C) and C-O (or C-OH) stretching were observed at 1706; 1507 and 1230 cm^{-1} respectively (13, 36). The absorption peak observed at 2954 cm^{-1} is characteristic for linear aliphatic C-H stretching. Chitosan showed characteristic absorption bands at 3362 and 2873 cm^{-1} due to aliphatic primary amine N-H symmetrical stretching vibrations and symmetric $-CH_2$ stretching vibration from the pyranose ring respectively (37). The absorption bands at 1651 and 1590 cm^{-1} are ascribed to primary amine, NH bend while 1025 and 1150 cm^{-1} peaks were due to primary amine C-N stretching and C-O-C antisymmetric bridge from the saccharide structure (Fig. 4b) (38). The spectra of Ibuprofen-Chitosan physical mixture exhibited the features of both components with no visible changes. New peak was observed in the IB-CT *nanoplex* at 1656–1632 cm^{-1} suggesting formation of an amide adduct (1680–1630 cm^{-1}) (13, 39). In the ibuprofen-chitosan nanoassembly, the characteristic carbonyl absorption peak at 1706 cm^{-1} in pure ibuprofen shifted to higher values with reduce intensity and broadened peak as CT concentration increased. The carbonyl peak disappeared completely at chitosan concentration 3.28×10^{-4} g/dm^3 and above supporting the interaction between ibuprofen and chitosan (Fig. 4).

Thermo-analytical Characteristics

The DSC thermogram of pure ibuprofen (Fig. 5a) showed a well-defined melting onset of 76.52±0.81°C (melting peak at 80.07±1.76°C; ΔH=29.77±1.89 J/g) corresponding to the reported valued in literature (75–78°C) (40, 41). The decomposition peak was observed at 234.45±7.11°C which corresponded to the mass loss at 235.80±4.09°C on TGA derivative curves (Fig. 6a). The amorphous chitosan exhibited T_g at 38.22±1.07°C and two degradation peaks at 106.55±3.38°C (endothermic) and 317.06±5.11°C (exothermic) respectively. The degradation peaks corresponded to large mass loss on TGA curves at the 311.76°C (Fig. 6b). Ibuprofen-chitosan physical mixture exhibited individual peaks of the components (Figs. 5c and 6c) with lower onset of melting at 73.38±0.88°C (peak at 78.03±1.04°C) but slightly higher delta H (ΔH=31.89±0.97 J/g). The ibuprofen-chitosan *nanoplex* exhibited three peaks (Fig. 5d–f) however the endothermic melting peak of ibuprofen was missing confirming the electrostatic interaction between ibuprofen and chitosan. The peak near zero degree was ascribed to the melting of ice crystals while those close to 100°C (104.35–105.20°C) were ascribed to evaporation of water. This assertion was confirmed in the TGA derivative curves as all *nanoplex* samples exhibited only one broad peak irrespective of chitosan concentration (Fig. 6d–f) indicating that a single eutectic amorphous product

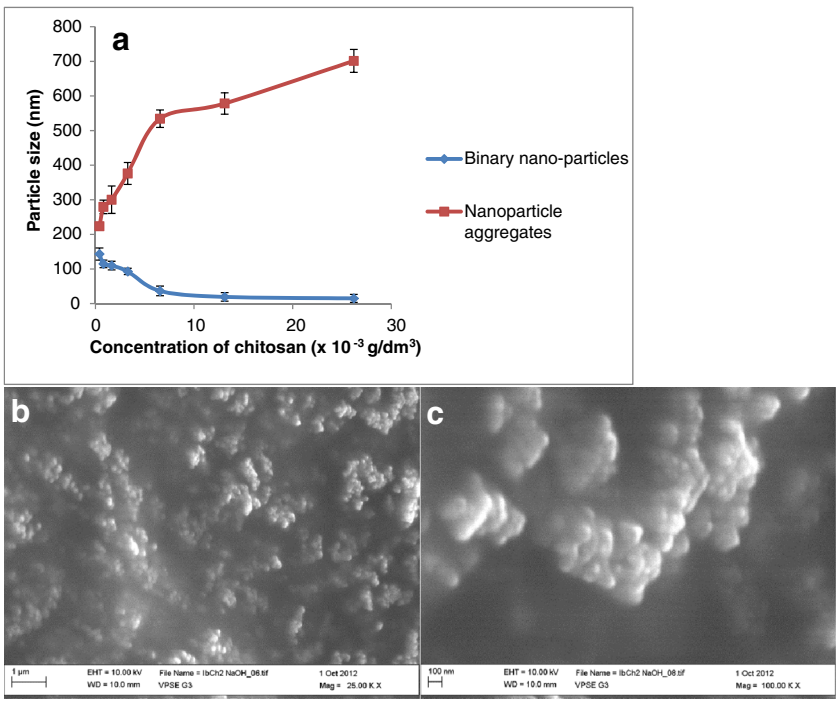

Fig. 3 Chitosan-induced changes in the size of ibuprofen nanoparticles (**a**) effect of CT concentration (26.24×10^{-3} g/dm^3) on the particle size of the *nanoplex* and its aggregates; aggregates of *nanoplex* at (**b**) × 25,000 and (**c**) × 100,000 magnification respectively.

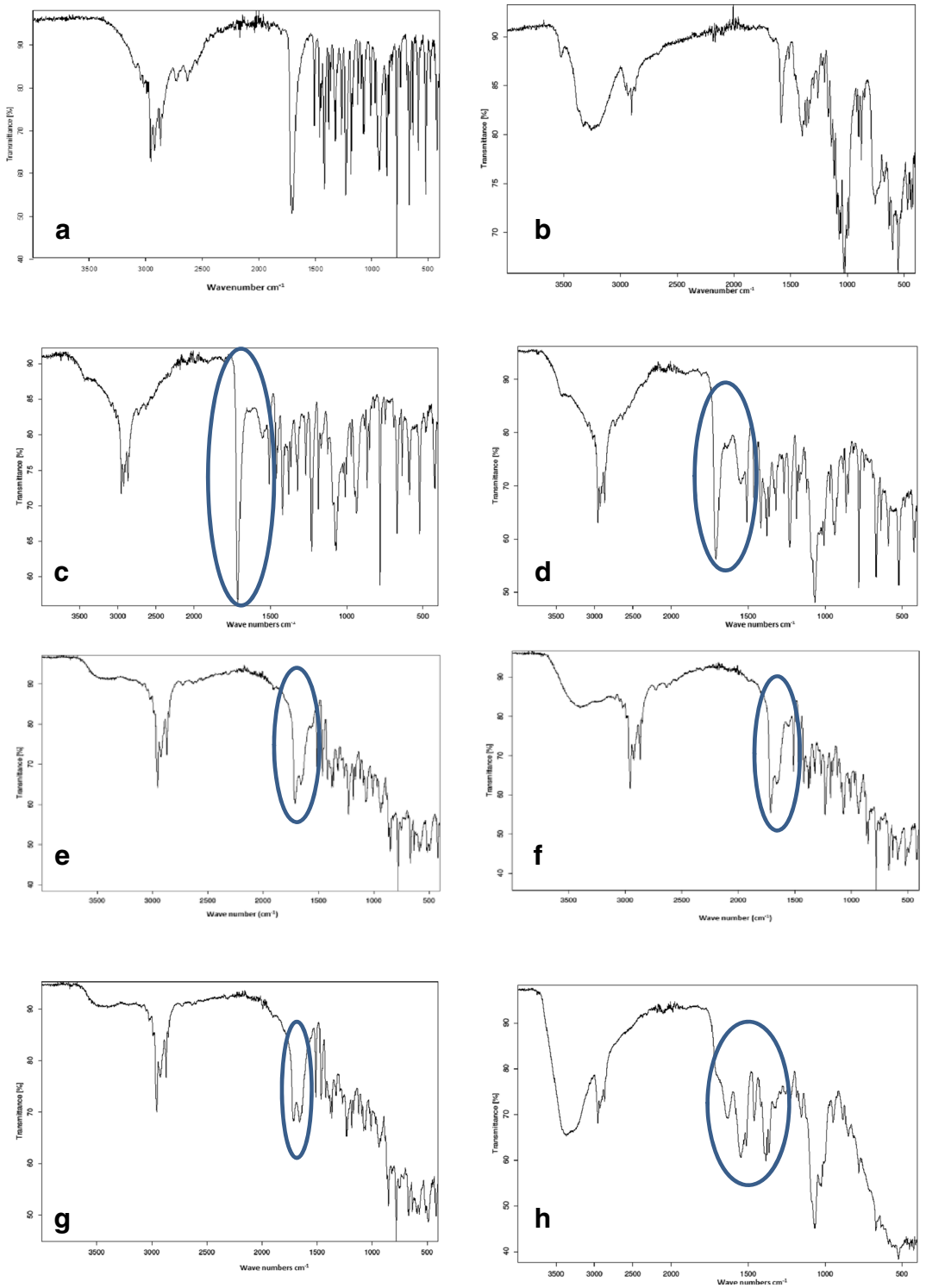

Fig. 4 FT-IR spectra of (**a**) pure ibuprofen; (**b**) chitosan powder; IB-CT *nanoplex* containing (**c**) 0.82; (**d**) 1.64 (**e**) 3.28; (**f**) 6.56; (**g**) 13.12 and (**h**) 26.24×10^{-3} g/dm^3 CT respectively.

was formed. The T_g of chitosan was not detected in any of the nanoplex samples suggesting permanent structural change. Also, the melting point of ibuprofen decreased remarkably with chitosan concentration, from 80.07 ± 1.76 to 56.90 ± 0.88°C ($p < 0.05$; $n = 6$) at 26.24×10^{-3} g/dm^3 chitosan, corresponding to 28.94% decrease in crystallinity of ibuprofen. We have reported similar binary amorphous ibuprofen-Ddex conjugate crystanules prepared by melt-*in situ* granulation-crystallizaton technique (4). The TGA curves of pure ibuprofen and the IB-CT *nanoplex*

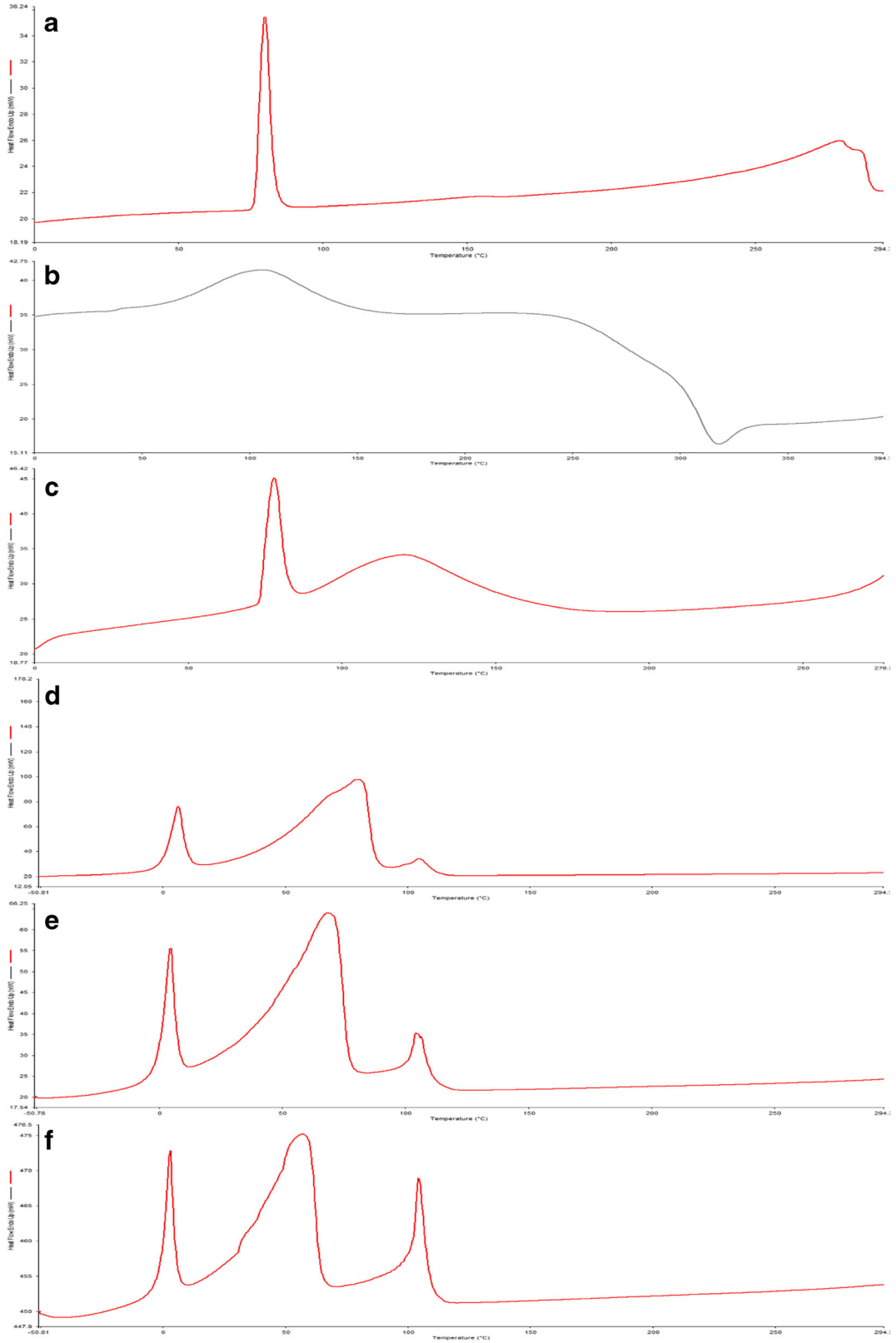

Fig. 5 DSC Thermograms of (**a**) pure ibuprofen; (**b**) chitosan powder; (**c**) ibuprofen-chitosan physical mixture and IB-CT *nanoplex* containing (**d**) 0.82; (**e**) 6.56 and (**f**) 26.24×10^{-3} g/dm^3 CT respectively.

exhibited a single step zero order degradation process (Fig. 6) which is consistent with the process described by Krupa *et al.* (42). The mass loss in the IB-CT *nanoplex* decreased to a minimum 73.14% with chitosan concentration

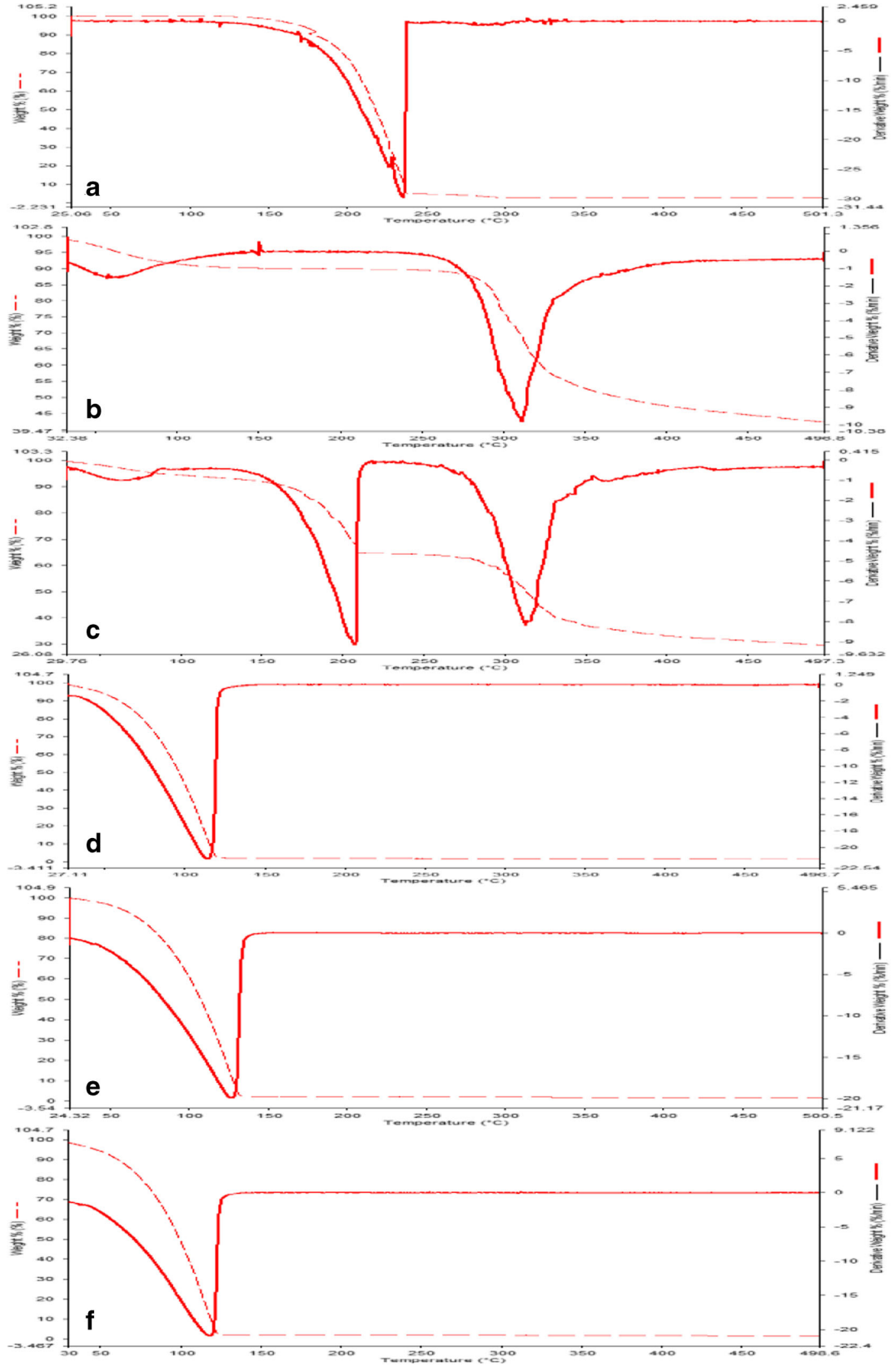

Fig. 6 Derivative TGA of (**a**) pure ibuprofen; (**b**) chitosan powder; (**c**) ibuprofen-chitosan physical mixture and IB-CT *nanoplex* containing (**d**) 0.82; (**e**) 6.56 and (**f**) 26.24×10^{-3} g/dm^3 CT respectively.

compared with pure ibuprofen (98.09%) suggesting improved thermal stability of the *nanoplex*.

Effect of Drug-Polymer Conjugation on Saturation Solubility Dynamics of Ibuprofen

The extent of intermolecular interaction between ibuprofen and chitosan may influence the intramolecular conformation and intermolecular close packing within the nanoplex and may impact the solubility characteristics of ibuprofen. In order to understand the molecular basis of the impact of IB-CT nanocomplexation on solvation process of ibuprofen, changes in the saturated solubility at different temperatures and solubility parameters of the *nanoplex* were investigated.

The ideal solubility of pure ibuprofen and the corresponding nanoplex was calculated using Eq. 10:

$$In\ X_2^{id} = -\frac{\Delta H_{fus}\left(T_{fus}-T\right)}{RT_{fus}T} + \left(\frac{\Delta S_{fus}}{R}\right)\left[\frac{\left(T_{fus}-T\right)}{T} + In\left(\frac{T}{T_{fus}}\right)\right] \quad (10)$$

where X_2^{id} is the ideal solubility of the solute in mole fraction; ΔH_{fus} and ΔS_{fus} are the molar enthalpy and entropy of fusion of the pure solute respectively; T_{fus} is the absolute melting point; T is the absolute temperature and R is the gas constant (43).

The experimental and ideal solubility parameters for the *nanoplex* are presented in Table I while the effects of temperature and CT concentration on solubility of IB are presented in Fig. 7. Solubility of ibuprofen increased steadily with CT concentration (Fig. 7a) to a maximum of 0.1256; 0.1167 and 0.1134 mg/ml corresponding to 3.31, 3.07 and 2.98 times increase at 18, 25 and 37°C respectively compared to pure ibuprofen with 0.038 mg/ml (log *S* of −3.268) as reported by Filippa and Gasull, (44). The *nanoplex* solubility profile exhibited breakpoints at maxima solubility values and the inflection points were determined from the intersection of the regression of the linear regions before and after the break points on the solubility curves. Only one inflection point was observed at 18°C (0.8189×10^{-3} g/dm^3 CT) and 25°C (1.6532×10^{-3} g/dm^3 CT) and was ascribed to the critical complexation concentration of CT where the IB-CT interaction commenced. At 37°C two inflection points were noted at 0.8189 and 6.55×10^{-3} g/dm^3 CT corresponding to multiple complexation at different polymer saturation point *(psp)* as temperature increased. The rate of solubilization and complexation constant (K_c) of the *nanoplex* as well as the intrinsic solubility of the uncomplexed ibuprofen were determined respectively from the slope and intercept of the solubility *versus* CT concentration graph as shown in Table I (45). K_c increased steadily with temperature suggesting greater affinity and bond strength in the IB-CT *nanoplex*. In a similar study, Khan *et al.*,

Table I Physicochemical Properties and Solubility Parameters of Pure Ibuprofen and IB-CT *Nanoplex*

Chitosan concentration ($\times 10^{-3}$ g/dm^3)	Experimental solubility (mole fraction)			[a]Ideal solubility (X_2^{id})			[b]Hildebrand solubility parameter (δ_H)		
	291 K	298 K	310 K	291 K	298 K	310 K	291 K	298 K	310 K
Pure ibuprofen	0.20 ± 0.0081	0.26 ± 0.0034	0.34 ± 0.0102	0.20 ± 0.0073	0.27 ± 0.0009	0.35 ± 0.0076	2.87 ± 0.0288	2.92 ± 0.0119	3.01 ± 0.0129
0.82	0.43 ± 0.0032	0.49 ± 0.0077	0.46 ± 0.0101	0.42 ± 0.0094	0.44 ± 0.0093	0.46 ± 0.0066	2.90 ± 0.0133	2.95 ± 0.0161	3.04 ± 0.0202
1.64	0.44 ± 0.0068	0.55 ± 0.0047	0.46 ± 0.0089	0.86 ± 0.0072	0.87 ± 0.0107	0.90 ± 0.0049	3.17 ± 0.0199	3.22 ± 0.0184	3.30 ± 0.0128
3.28	0.47 ± 0.0066	0.58 ± 0.0091	0.48 ± 0.0074	0.96 ± 0.0085	0.98 ± 0.0102	0.86 ± 0.0162	3.20 ± 0.0201	3.25 ± 0.0185	3.33 ± 0.0192
6.56	0.49 ± 0.0065	0.55 ± 0.0074	0.57 ± 0.0097	0.82 ± 0.0076	0.83 ± 0.0079	0.85 ± 0.0096	3.39 ± 0.0118	3.44 ± 0.0183	3.51 ± 0.0097
13.12	0.55 ± 0.0077	0.54 ± 0.0033	0.47 ± 0.0019	0.81 ± 0.0091	0.82 ± 0.0056	0.84 ± 0.0069	3.47 ± 0.0119	3.51 ± 0.0214	3.58 ± 0.0198
26.24	0.63 ± 0.0042	0.51 ± 0.0061	0.47 ± 0.0055	0.75 ± 0.0097	0.77 ± 0.0086	0.76 ± 0.0064	3.50 ± 0.0059	3.54 ± 0.0148	3.61 ± 0.0108
[c]Intrinsic saturated solubility (mg/ml)	0.08 ± 0.0095	0.09 ± 0.0067	0.73 ± 0.0098	0.31 ± 0.0089	0.32 ± 0.0059	0.34 ± 0.0091			
[c]Complexation constant ($K_c\times10^{-2}$)	4.50 ± 0.0201	7.80 ± 0.0218	17.29 ± 0.0487	6.48 ± 0.0273	7.20 ± 0.0228	15.46 ± 0.0418			
[c]Rate of solubilisation	0.0037 ± 0.0002	0.0073 ± 0.0001	0.1120 ± 0.0008	0.0198 ± 0.0003	0.0226 ± 0.0001	0.0496 ± 0.0004			

[a] Ideal solubility was calculated from Eq. 10

[b] Hildebrand solubility parameters were derived from Eq. 11

[c] Intrinsic saturated solubility, complexation constant and rate of solubilization were derived from solubility phase diagrams

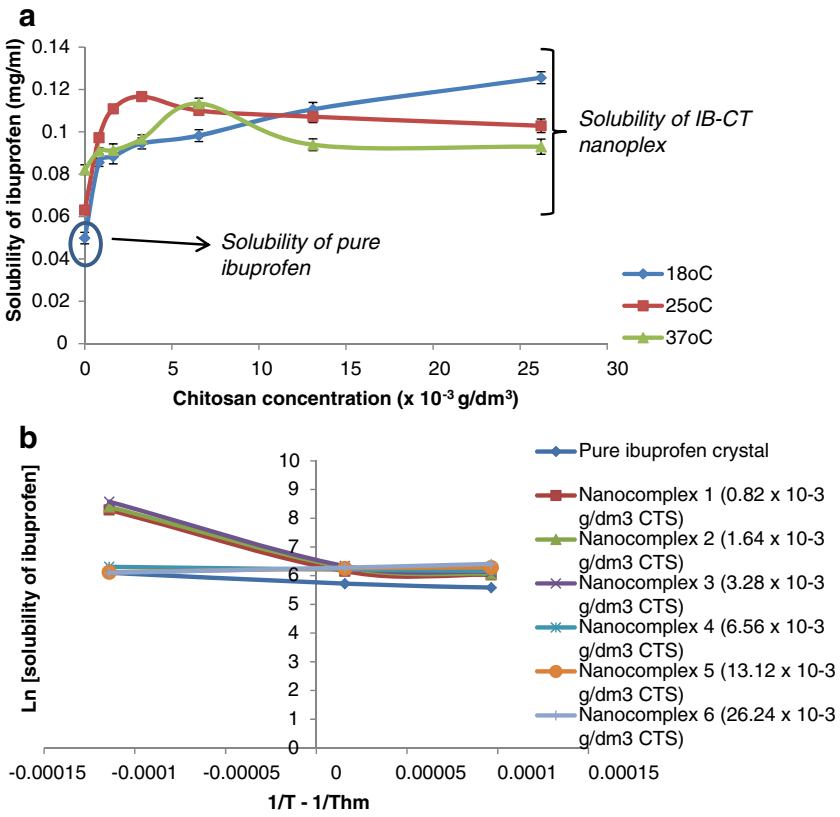

Fig. 7 Phase solubility diagram of nanoplex at different CT concentration and temperature (*Thm =299.463 K*).

(14) reported a reduction in critical association concentration (*cac*) of ibuprofen sodium as evidence of strong affinity between ibuprofen and a cationic polymer, hydroxyethyl cellulose ethoxylate quaternized (HECEQ). Since the *cac* increased with temperature during the process of solubilisation in this study, it was concluded that affinity between IB and CT decreased significantly with temperature which may account for the higher solubility of the nanoplex compared to pure ibuprofen. However the adhesive properties of CT as shown in the SEM data have limited this phenomenon.

The slope of the linear region of the phase solubility diagrams were less than unity in all cases suggesting formation of higher order complexes with respect to CT. Also, deviation of solubility curves from linearity at higher CT concentration indicates the existence of a non-ideal process of solvation and that multiple complexes were formed as concentration of CT increased. This is consistent with our previous report on ibuprofen-Ddex conjugates (6). Solubility increased with temperature at low concentration of CT however the order was reversed above 6.56×10^{-3} g/dm^3 CT where solubility at 18°C>25°C>37°C respectively (Fig. 7b). This is in contrast to our findings with Ddex which exhibited extended solubility at high temperature, probably due to strong adhesive property of CT which may have been enhanced by heat. All the temperatures used in this study are lower than the glass transition temperature (T_g) of CT (38.22°C). At these temperatures, the *nanoplex* would be in glassy state where structural mobility is very low hence the diffusion rate of ibuprofen through the nanoparticle complex was limited. The slight reduction of solubility at higher CT concentrations and temperature may be explained by the profound influence of various intermolecular interactions between IB and CT on solute-solvent solubilisation process. The predicted ideal solubility was higher than the experimental results especially at higher concentration of CT suggesting that solute-solvent solubility behaviour cannot be explained by enthalpy of fusion and entropy alone especially in drug-polymer conjugate design. Other factors such as chemical properties of the drug (cohesiveness), drug-polymer intermolecular interaction (solute-solute), hydrogen bonding, polymer characteristics, chemical properties of the solvent, solute-solvent interaction, dispersion forces, dipole moment, etc., may have profound influence of solubility profile.

In order to study the role of IB-CT complexation on the self-cohesive characteristic of ibuprofen, Hildebrand's solubility parameter (δ_H), defined as the square root of cohesive energy density, was calculated from Hildebrande and Hansen solubility parameters (Eq. 11) (46) and presented in Table I:

$$\delta_H = \sqrt{\left(\frac{\Delta H_{vap} - RT}{V}\right)} \tag{11}$$

where ΔH_{vap} is the enthalpy of vapourization; V is the molar volume; R and T are gas constant and absolute solution temperature respectively.

Table II Estimation of Molar Volume, Hansen Partial Solubility Parameters and Hildebrand Total Solubility Parameters for Ibuprofen

Group in ibuprofen molecule	Quantity	*Molar volume*[a] ΔV (cm^3mol^{-1})	*Dispersion parameter* δ_d, ($J^{1/2}cm^{3/2}mol^{-1}$)	*Polar solubility parameter* [b] δ_p($J\ cm^3mol^{-2}$)	*Hydrogen bonding parameter,* δ_h($J\ mol^{-1}$)
−COOH	1	1 × 28.5	1 × 530	$(1\times420)^2$	1 × 10,000
Phenylene (*o, p-substituted benzene ring*)	1	1 × 52.4	1 × 1270	$(1\times110)^2$	1 × 0
>CH-	2	2 × −1.0	2 × 80	$(2\times0)^2$	2 × 0
$>CH_2$	1	1 × 16.1	1 × 270	$(1\times0)^2$	1 × 0
$-CH_3$	3	3 × 33.5	3 × 420	$(3\times0)^2$	3 × 0
TOTAL		195.5	3490	188,500	10,000
Partial solubility parameters			δ_d = 3490/195.5 = 17.9 $MPa^{1/2}$	$\delta_p = (188{,}500)^{1/2}/195.5 = 2.2\ MPa^{1/2}$	$\delta_h = (10{,}000/195.5)^{1/2} = 7.2\ MPa^{1/2}$
Total solubility parameter	$(17.9^2+2.2^2+7.2^2)^{1/2} = 19.42\ MPa^{1/2}$				

[a] Molar volume (ΔV) calculated from data reported by Fedors, 1974. Dispersion parameter (δ_d), polar solubility parameter (δ_p) and hydrogen bonding (δ_h) were calculated from the data reported by Barton, 1991

Table III Thermodynamic Functions of Solubilization Process of Pure Ibuprofen and IB-CT Nanoplex

Chitosan concentration ($\times 10^{-3}$ g/dm^3)	ΔH_{sol}($kJmol^{-1}$)	ΔH_{fus}($kJ\ mol^{-1}$)[b]	T_{fus}(K)[b]	ΔS_{sol}($JK^{-1}mol^{-1}$)	[a] ΔG_{sol}($kJmol^{-1}$) *van't Hoff equation*	[b] ΔG_{sol} ($kJmol^{-1}$)[a] ($\Delta G = \Delta H - T\Delta S$)	[c] ΔG_{sol} ($kJmol^{-1}$) ($\Delta G = -2.303RT\ log[S_0/S_S]$)	ζH%	ζS%	R^2
Pure ibuprofen	20.728 ± 0.111	25.50	347.15	48.23 ± 1.056	−14.44 ± 0.208	−14.42 ± 0.114	–	58.94	41.06	0.9837
0.82	23.74 ± 0.421	67.62	348.60	56.67 ± 0.957	−16.97 ± 0.206	−16.88 ± 0.119	−37.805 ± 0.661	84.67	15.33	0.9892
1.64	26.24 ± 0.166	170.12	319.84	57.42 ± 1.004	−17.19 ± 0.194	−17.10 ± 0.314	−40.433 ± 0.209	84.84	15.16	0.9120
3.28	31.16 ± 0.172	414.46	314.22	58.25 ± 0.811	−17.44 ± 0.107	−17.34 ± 0.231	−44.999 ± 0.630	85.29	14.71	0.9057
6.56	5.71 ± 0.260	455.04	313.08	57.78 ± 1.196	−15.61 ± 0.261	−15.61 ± 0.109	−16.445 ± 1.003	76.91	23.09	0.9951
13.12	−6.67 ± 0.217	771.67	313.00	52.09 ± 1.301	−15.51 ± 0.201	−15.50 ± 0.406	−16.206 ± 0.512	61.75	38.25	0.9594
26.24	−12.20 ± 0.198	805.58	312.78	51.71 ± 1.286	−15.49 ± 0.166	−15.49 ± 0.160	−11.514 ± 0.714	55.81	44.19	0.9979

ΔH_{sol} and ΔS_{sol} were calculated from the slope and intercept while [a] ΔG_{sol} was determined from the intercept at harmonic temperature (T_{hm} = 322.129 K) of van't Hoff equation (Eq. 12); [b] ΔG_{solb} was calculated from $\Delta G = \Delta H - T\Delta S$; ζH% and ζS% are relative contributions of enthalpy and entropy towards Gibbs free energy of solubilization, the values were calculated using Eqs. 16 and 17 respectively. [c] ΔG_{sol} was calculated at 37°C (310 K) using Costa's equation $\Delta G = -2.303RT\ log[S_0/S_S]$. Molar enthalpies of fusion (ΔH_{fus}) at melting point and absolute melting point (T_{fus}) obtained from Perlovich *et al.*, 2004

Molar volume of ibuprofen was estimated from the Fedors and van Krevelen techniques (47, 48) as shown in Table II. It was evident that the dispersion forces were more prominent in ibuprofen with significant contributions from the di-substituted benzene (*phenylene)* ring and methyl groups. The total solubility parameter (δ_H) of 19.42 $MPa^{1/2}$ indicates that ibuprofen could be classified as semi polar and solvents with similar δ_H should produce the greatest solubility (48). As shown in Table I, the δ_H of pure IB were 2.87, 2.92 and 3.01 K at 291, 298 and 310 K respectively slightly higher than the reported δ_H for ibuprofen in water (δ_H=2.294; (44)). The δ_H for IB-CT *nanoplex* increased with CT concentration and temperature indicating increasing polarity relative to pure IB however the difference was not statistically significant among

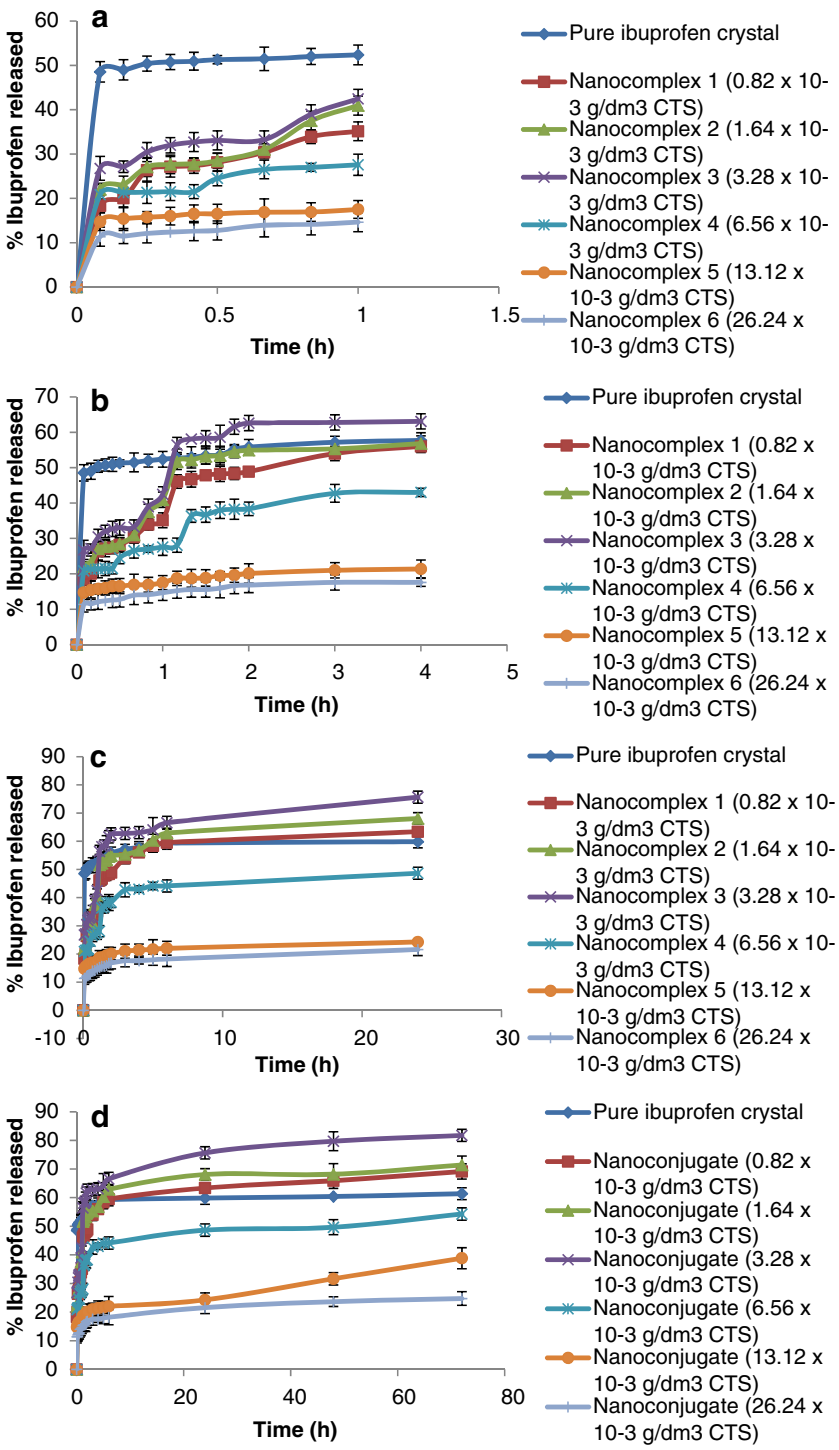

Fig. 8 Time-dependent extended release of ibuprofen from the nanocomplex at (**a**) 1 h; (**b**) 4 h; (**c**) 24 h and (**d**) 72 h.

the *nanoplex* batches ($p>0.05$, $n=6$). Also, distilled water, used as the solvent in this study, has high polarity and hydrogen bond acceptance capacity which may limit dipolar solute-solvent interaction at high concentration of CT, resulting in low solubility of IB. In theory when water molecules surround the polar carboxylic group of ibuprofen, solvation energy is released to facilitate its solubilisation. However the absence of free carboxylic group in the eutectic IB-CT *nanoplex*, as shown in the FTIR and DSC data, may limit this process.

Thermodynamic Analysis of IB-CT Nanoplex Solubilization Process

The mechanism of solvation of IB-CT nanoplex in distilled water was evaluated by determining enthalpy, entropy and Gibbs free energy changes from the plots of van't Hoff thermodynamic equation as described by Filippa and Gasull (44) (Eq. 12).

$$ln\ S = \frac{-\Delta H}{RT} + \frac{\Delta S_{sol}}{R} \tag{12}$$

where S is the molar solubility of ibuprofen in the conjugate system; T is the absolute solution temperature (K), R is the universal gas constant while ΔH and ΔS_{sol} are the enthalpy and entropy for the solution process respectively.

ΔH and ΔS_{sol} were determined from the slope ($-\Delta H/R$) and intercept ($\Delta S_{sol}/R$) respectively of the *Ln S versus* $1/T$ plots and the harmonic temperature (T_{hm}) was used in the calculation of thermodynamic parameters in order to minimize intrinsic errors.

$$T_{hm} = \frac{n}{\sum_{n=1}^{n}(1/T)} \tag{13}$$

Table III shows the thermodynamic solubilisation parameters for pure ibuprofen in the IB-CT *nanoplex*. The enthalpy of solution (ΔH_{sol}) for pure ibuprofen was positive (20.73 kJmol^{-1}) which increased in the *nanoplex*, with CT concentration, to a maximum of 31.16 kJmol^{-1} at 3.28×10^{-3} g/dm^3 CT, followed by a remarkable decrease to negative values at high concentration of CT. This suggests that IB-CT interaction may have converted the endothermic and non-spontaneous process of dissolving IB in water into an exothermic and spontaneous process at higher concentration of CT which may explain the decreasing effect of temperature on solubility. The entropy of solution was positive in all cases and increased to a maximum with CT concentration similar to the enthalpy parameter. This suggests that the IB-CT-water systems became less ordered during the process of solubilisation, transiting from an ordered microenvironment to a more disordered bulk in the *nanoplex*. In theory this should translate to corresponding increase in solubility however the adhesive property of CT seemed to limit this phenomenon. The Gibbs free energy change of solution (ΔG_{sol}) was calculated at T_{hm} using Eq. 14 (49).

$$\Delta G_{sol} = -RT_{hm} \times Intercept \tag{14}$$

The Gibbs free energy *was* negative in all cases (Table III) suggesting spontaneous solubilization process. The ΔG_{sol} and other thermodynamic parameters calculated using the conventional equation ($\Delta G = \Delta H - T\Delta S$) was consistent with the values obtained from the van't Hoff's model however ΔG_{sol} derived from Costa's equation (24) increased to a maximum of -44.999 ± 0.630 kJmol^{-1} followed by a steady decrease with CT concentration, consistent with solubility profile.

$$\Delta G = -2.303RT\ \ Log[S_0/S_S] \tag{15}$$

where $[S_0/S_S]$ is the ratio of the molar solubility of ibuprofen before and after conjugation. The value of gas constant R is 8.314 J K^{-1} mol^{-1} and T is temperature in degree kelvin (299.463 K).

The relative contributions of the enthalpy ($\zeta H\%$) and entropy ($\zeta S\%$) toward the Gibbs free energy of solubilization were calculated using the following equations and presented in Table III (44):

$$\zeta H\% = \left[\frac{|\Delta H_{solb}|}{|\Delta H_{solb}| + |T\Delta S_{solb}|}\right]100 \tag{16}$$

$$\delta S\% = \left[\frac{|T\Delta S_{solb}|}{|\Delta H_{solb}| + |T\Delta S_{solb}|}\right]100 \tag{17}$$

Overall, the percentage contribution of enthalpy was higher than entropy term however entropic contribution increased at higher concentrations of CT suggesting a gradual change from enthalpy driven to entropy driven solubilization process (Table III).

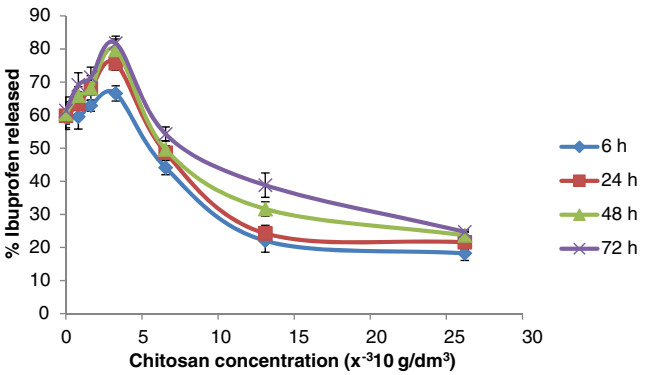

Fig. 9 Effect of chitosan concentration on *in vitro* release kinetics of ibuprofen from nanocomplex.

Dissolution Studies

The *in vitro* release kinetics of ibuprofen from the IB-CT *nanoplex* is presented in Fig. 8. Pure ibuprofen exhibited initial burst release of 48.54% at 5 min compared with 11.36–26.77% in the *nanoplex* indicating controlled release phenomenon. Within the first 1 h the extent of release from pure IB was greater than all the *nanoplex* batches. In corollary, after I h the percent drug released from the *nanoplex* decreased significantly ($p<0.05$; $n=6$) with CT concentration from 52.38% (pure IB) to 14.64% in *nanoplex* containing 26.24×10^{-3} g/dm^3 CT (Fig. 8a). Within 4 h IB-CT *nanoplexes* exhibited extended release pattern (Fig. 8b)and the batch containing 3.28×10^{-3} g/dm^3 CT exhibited greater IB release (63.08%) than IB (57.72%). After 24 h, all *nanoplex* containing low concentrations of CT up to 3.28×10^{-3} g/dm^3 exhibited extended release greater than pure IB (Fig. 8c) which is consistent with the solubility data. Figure 8d also shows continuous extended release of IB from all the *nanoplex* batches up to 72 h. Overall increasing concentration of CT increased dissolution rate to a maximum at 3.28×10^{-3} g/dm^3 followed by a steady retardation (Fig. 9). It was evident that higher concentrations of CT retarded dissolution rate significantly due to its intermolecular interaction with IB and its adhesive properties as well as the physical aggregation of the nanoparticle complex as shown in the SEM data. However extended dissolution rate of the *nanoplex* was ascribed to the remarkably reduced particle size to nanometre range and conversion of the crystalline IB into amorphous powder. In similar studies DEAE Dextran and silicon dioxide have been reported to increase dissolution of ibuprofen from 52.4 to 100% (5) and from 46 to 77% (50) respectively. The enhanced dissolution of ibuprofen at low concentrations of CT was ascribed to disruption of the crystalline structure of IB, conversion to amorphous state and particle size reduction as shown in the DSC and SEM data of this report.

IB has a short biological half-life (2 h) and complete excretion usually occurs within 24 h, therefore dissolution parameters were determined at 2 and 72 h to mimic the half-life and maximum drug release respectively. Within 2 h, MDT and DE of the *nanoplex* increased to maximum values of 0.57 h and 62.60% respectively at 3.28×10^{-3} g/dm^3 CT followed by steady decrease (Table IV). Increased mean dissolution time (MDT) indicates reduced dissolution rate with time due to saturation of the dissolution medium, which is consistent with MDR results in Table IV. Increase in DE also demonstrates the dissolution enhancing capacity of CT. The variance of dissolution time (VT) and time required for 50% dissolution (T_{50}) increased steadily with CT concentration indicating that variability was low below the critical complexation concentration of CT while dissolution efficiency was higher. Higher concentrations of CT decreased DE, MDR and MDT providing evidence for the extended release profile. The difference factor (f_1) increased from 13.92 to 70.40% while the similarity factor (f_2) decreased from 43.70 to 21.29% indicating highly significant dissimilarity between IB and the *nanoplex* as f_2 values are less than 50% at all concentrations of CT (Table IV). The minimum f_1 (4.09%) and maximum f_2 (43.70%) were obtained at 3.28×10^{-3} g/dm^3 CT corresponding to the critical complexation concentration and consistent with other findings in this study. It was evident that lower concentrations of CT exhibited high drug release capacity with potential application as rapid dissolving formulation while higher concentrations exhibited retarded dissolution velocity with potential application in extended release strategy for IB. It was concluded that the overall rate and extent of ibuprofen dissolution profiles cannot be explained exclusively by size reduction.

Mechanism of Ibuprofen Release from the Nanoplex

Table V shows the parameters for mechanism of ibuprofen release from the *nanoplex*. Pure ibuprofen reference fitted fairly into first order ($R^2=0.9373$); Higuchi ($R^2=0.9730$) and Korsmeyer-Peppas ($n=0.40$; $R^2=0.9258$) but did not fit into zero order and Hixson-Crowell mathematical equations

Table IV Dissolution Parameters Calculated from Mathematical Equations for IB-CT *Nanoplex*

Chitosan concentration ($\times 10^{-3}$ g/dm^3)	Conjugation efficiency (%)	MDT (h)		MDR (%h^{-1})		DE (%)		VT (h)^2	T_{50}	Dissimilarity and similarity factors		
		MDT_{2h}	MDT_{72}	MDR_{2h}	MDR_{72}	DE_{2h}	DE_{72h}	VT_{2h}	T_{50} (h)	f_1	f_2	Correlation coefficient
Pure ibuprofen	–	0.16	1.77	1.10	0.84	55.82	61.38	0.154	0.21	–	–	
0.82	10.57 ± 0.7137	0.49	4.77	4.71	3.54	48.88	69.15	0.207	1.22	19.70	40.33	$R^2=0.9509$
1.64	25.78 ± 1.5070	0.52	5.83	4.04	2.99	54.94	71.42	13.16	1.31	13.92	42.38	$R^2=0.9586$
3.28	49.43 ± 1.3786	0.57	9.14	3.69	2.71	62.60	81.76	16.35	1.55	4.09	43.70	$R^2=0.9412$
6.56	70.23 ± 3.4011	0.48	8.10	1.60	1.26	38.38	54.30	15.70	2.92	36.85	33.78	$R^2=0.9423$
13.12	96.67 ± 8.4838	0.32	7.69	0.84	0.65	20.11	38.84	13.753	13.39	62.96	23.42	$R^2=0.9719$
26.24	98.75 ± 5.6619	0.27	5.63	0.68	0.52	16.82	24.74	14.75	13.39	70.49	21.29	$R^2=0.9714$

Table V Mechanisms of Ibuprofen Release from the *Nanoplex*

Dissolution mathematical models	Zero order kinetics			First order kinetics			Higuchi model			Hixson-Crowell model			Korsmeyer-Peppas model		
Equation	$Q_t = Q_0 + K_0 t$			$Q_t = Q_0 e^{-K_1 t}$			$Q = K_H t^{1/2}$			$W_0^{1/3} - W_t^{1/3} = K_s t$			$Mt / M_\infty = at^n$		
Mechanism of release	Constant rate of release			Diffusion (Fick's first law)			Diffusion and permeability			Erosion release			Diffusion (semi empirical model)		
Chitosan concentration ($\times 10^{-3}$ g/dm^3)	[a]Q_0	[c]K_0	[b]R^2	[a]Q_0	[d]K_1	[b]R^2	[a]Q_0	[e]K_H	[b]R^2	[a]W_0	[f]K_s	[b]R^2	[g]n	[h]b	[b]R^2
Ibuprofen powder	50.13	0.0334	0.8859	1.6942	0.0004	0.9373	47.501	0.6561	0.9730	3.6702	0.0011	0.8888	0.40	1.6551	0.9258
0.82	18.19	0.3420	0.9509	1.3012	0.0046	0.9292	8.765	3.8764	0.9494	2.6943	0.0111	0.9419	1.0812	1.5793	0.9566
1.64	18.81	0.3980	0.9586	1.3225	0.0050	0.9716	8.019	4.4909	0.9397	2.7467	0.012	0.9684	0.7054	1.4989	0.9595
3.28	24.06	0.1515	0.9412	1.3998	0.0043	0.9512	10.522	4.7738	0.9166	2.9359	0.0101	0.9457	0.5944	1.4938	0.9561
6.56	18.72	0.1785	0.9423	1.2958	0.0027	0.9474	12.359	2.3329	0.9197	2.6904	0.0063	0.9468	0.5476	1.4569	0.9398
13.12	15.06	0.0435	0.9719	1.1807	0.0011	0.9634	13.419	0.6622	0.9785	2.4733	0.0021	0.9666	0.5371	1.0812	0.9638
26.24	11.45	0.0480	0.9714	1.0493	0.0020	0.9759	13.511	0.5819	0.9873	2.2554	0.0029	0.9619	0.4969	1.4760	0.9816

Profiles with minimum dissolution rate greater than 60% were not determined

[a] Q_0, W_0 intrinsic dissolution

[b] R^2 ,coefficient of determination

[c] K_0 zero order release rate constant

[d] K_1 first order release rate constant

[e] K_H Higuchi's diffusion rate constant

[f] K_s Hixson-Crowell's diffusion rate constant

[g] n Korsmeyer Peppas' release exponent

[h] b Korsmeyer-Peppas' measure of burst effect

suggesting diffusion mechanism of release. All the IB-CT *nanoplexes* fitted fairly well into all the mathematical models used in this study suggesting a combination of various release mechanisms. Good fitness into zero order indicate constant slow (prolonged) drug release from matrix and osmotic delivery systems where there is no disaggregation and the specific surface area remains constant (18). Although the decrease in intrinsic dissolution efficiency (Q_o) provide evidence for the prolonged release capacity of the *nanoplex*, the zero order release rate constant (K_0) was not constant at higher concentrations of CT suggesting that fitness of drug release into mathematical models cannot be completely described exclusively by correlation of determination. In first order kinetics, drug release is proportional to the amount of drug remaining in the matrix such that drug release decrease with time. The first order release rate was significantly higher (3–13 times) in the *nanoplex* (0.0011–0.0050 h^{-1}) than IB reference (0.0004 h^{-1}) and the intrinsic dissolution efficiency decreased with CT concentration due to intermolecular interaction between IB and CT, providing evidence for the concentration-dependent release mechanism in the *nanoplex*. Higuchi's diffusion rate constant increased to a maximum followed by a steady decrease while the intrinsic dissolution efficiency increased steadily with CT concentration suggesting release of water soluble drug from matrix delivery system by diffusion (51). It was opined that conversion of IB crystals into amorphous nanostructures has improved its hydrophilicity facilitating diffusion through the *nanoplex* matrix. Hixson-Crowell model assumes that the rate of drug release is limited by dissolution of drug particles not by diffusion. Fitness of the *nanoplex* into this model may be explained by potential aggregation of the nanoparticle complex at higher concentration of CT as shown in the SEM data. Both IB reference and the *nanoplex* fitted well into Korsmeyer-Peppas' model indicating diffusion of drug from controlled-release polymeric system determined within < 60% dissolution rate. The release exponent (n) for the IB-CT *nanoplexes* decreased steadily with CT concentration from 1.0812 at 0.82×10^{-3} to 0.497 at 26.24×10^{-3} g/dm^3 compared with IB reference (0.40) suggesting change in mechanism of release from Super Case II transport through anomalous transport to Fickian diffusion in the *nanoplex*. It was concluded that multiple mechanisms are involved in the release of ibuprofen from the nanoparticle complex however diffusion was predominant.

CONCLUSION

This study investigated the direct effect of intermolecular interaction of ibuprofen with chitosan on crystal behaviour, saturated solubility and dissolution efficiency of ibuprofen. The interaction produced amorphous nanoparticle complex (*nanoplex*) which enhanced the saturated solubility and dissolution velocity of IB at low CT concentrations. The nanoplex exhibited both fast and extended release profiles dictated by CT concentrations. This study demonstrated the potential application of drug-polymer nanocomplex design in multi-functional regulated drug delivery.

ACKNOWLEDGMENTS AND DISCLOSURES

We thank Mrs Elizabeth O'Brien, Leicester School of Pharmacy, for her precious time during SEM analysis.

REFERENCES

1. Luo Y, Wang Q. Recent development of chitosan-based polyelectrolyte complexes with natural polysaccharides for drug delivery. Int J Biol Macromol. 2014;64:353–67.
2. Najafabadi AH, Abdouss M, Faghihi S. Synthesis and evaluation of PEG-O-chitosan nanoparticles for delivery of poor water soluble drugs: ibuprofen. Mater Sci Eng C. 2014;41:91–9.
3. Florence AT, Attwood D. Physicochemical principles of pharmacy. 3rd ed. London: Macmillan; 1998. p. 199–251.
4. Abioye A, Kola-Mustapha A, Ruparelia K. Impact of insitu granulation and temperature quenching on crystal habit and micromeritic properties of ibuprofen-cationic dextran conjugate crystanules. < br /> Int J Pharm. 2014;462(1–2):83–102.
5. Abioye A, Kola-Mustapha A, Chi GT, Iliya S. Quantification of in situ granulation-induced changes in pre-compression, solubility, dose distribution and intrinsic in vitro release characteristics of ibuprofen-cationic dextran conjugate crystanules. Int J Pharm. 2014;471(1–2):453–77.
6. Abioye A, Kola-Mustapha A. Controlled electrostatic self-assembly of ibuprofen-cationic dextran nanoconjugates prepared by low energy green process - a novel delivery tool for poorly soluble drugs. Pharm Res. 2015;32:2110–31.
7. Abioye A, Kola-Mustapha A. Formulation studies on ibuprofen sodium-cationic dextran conjugate: effect on tableting and dissolution characteristics of ibuprofen. Drug Dev Ind Pharm. 2015b.
8. Abioye A, Issah S, Kola-Mustapha A. Ex vivo skin permeation and retention studies on chitosan-ibuprofen-gellan ternary nanogel prepared by in situ ionic gelation technique - a tool for controlled transdermal delivery of ibuprofen. Int J Pharm. 2015;490:112–30.
9. Rodríguez R, Alvarez-Lorenzo C, Concheiro A. Influence of cationic cellulose structure on its interactions with sodium dodecylsulfate: implications on the properties of the aqueous dispersions and hydrogels. Eur J Pharm Biopharm. 2003;56:133–42.
10. Rodríguez R, Alvarez-Lorenzo C, Concheiro A. Interaction of ibuprofen with cationic polysaccharides in aqueous dispersions and hydrogels: rheological and diffusional implications. Eur J Pharm Sci. 2003;20:429–38.
11. Torchilin VP, Lukyanov AN, Gao Z, Papahadjopoulos-Sternberg B. Targeted pharmaceutical carriers for poorly soluble drugs. Proc Natl Acad Sci. 2003;100:6039–44.
12. Vieira AP, Badshah S, Airoldi C. Ibuprofen-loaded chitosan and chemically modified chitosans – release features from tablet and film forms. Int J Biol Macromol. 2013;52:107–15.
13. Nokhodchi A, Amire O, Jelvehgari M. Physico-mechanical and dissolution behaviours of ibuprofen crystals crystallized in the presence of various additives. DARU. 2010;18(2):74–83.
14. Khan IA, Anjum K, Ali MS, Din K. A comparative study of interaction of ibuprofen with biocompatible polymers. Colloids Surf B: Biointerfaces. 2011;88:72–7.

15. Huh C, Mason SG. Rigorous theory of ring tensiometry. Colloid Polym Sci. 1975;253:566–80.
16. Lunkenheimer K, Wantke KD. On the applicability of the du Noüy (ring) tensiometer method for the determination of surface tensions of surfactant solutions. J Colloid Interface Sci. 1978;66(3):579–81.
17. Connors RD, Elder EJ. Delivery of poorly soluble or poorly permeable drugs. 4th ed. Fall Church: Technology Catalyst International Incorporation; 2003.
18. Costa P, Lobo JMS. Modeling and comparison of dissolution profiles. Eur J Pharm Sci. 2001;13:123–33.
19. Pillay V, Fassihi R. Evaluation and comparison of dissolution data derived from different modified release dosage forms: an alternative method. J Control Release. 1998;55(1):45–55.
20. Siepmann J, Siepmann F. Mathematical modelling of drug delivery. Int J Pharm. 2008;364:328–43.
21. Moore JW, Flanner HH. Mathematical comparison of dissolution profiles. Pharm Tech. 1996;20(6):64–74.
22. CDER F. Centre for Drug Evaluation and Research (CDER) at the Food and Drug Administration (FDA). SUPAC. 1995.
23. CDER F. Centre for Drug Evaluation and Research (CDER) at the Food and Drug Administration (FDA). IVIVC 1996.
24. Costa P. An alternative method to the evaluation of similarity factor in dissolution testing. Int J Pharm. 2001;220(1–2):77–83.
25. Yandell BS. Practical data analysis for designed experiments. FL: Chapman and Hall; 1997.
26. Yuksel N, Kanik AE, Baykara T. Comparison of in vitro dissolution profiles by ANOVA-based model-dependent and –independent methods. Int J Pharm. 2000;209(1–2):57–67.
27. Hadgraft JVC. PH, pKa and dermal delivery. Int J Pharm. 2000;200:243–7.
28. Potta SG, Minemi S, Nukala RK, Peinado C, Dimitrios A, Lamprou DA, *et al.*
Preparation and characterization of ibuprofen solid lipid nanoparticles with enhanced solubility. J Microencapsul. 2011;28(1):74–81.
29. Romero AJ, Savastano L, Rhodes CT. Monitoring crystal modifications in systems containing ibuprofen. Int J Pharm. 1993;99:125–34.
30. Ridell A, Evertsson H, Nilsson S, Sundel f LO. Amphiphilic association of ibuprofen and two nonionic cellulose derivatives in aqueous solution. J Pharm Sci. 1999;88(11):1175–81.
31. Khan IA, Anjum K, Koya PA, Kabir-ud-Din. Tensiometric and conductometric studies of the effect of polymers on the aggregation behaviour of cationic amphiphilic drugs IMP and PMT. J Mol Liq. 2014;193:6–12.
32. Jiang B, Hu L, Gao C, Shen J. Crosslinked polysaccharide nanocapsules: preparation and drug release properties. Acta Biomater J. 2005;2:9–18.
33. Galindo-Rodriguez SA, Puel F, Briancon S, Allemann E, Doelker E, Fessi H. Comparative scale-up of three methods for producing ibuprofen-loaded nanoparticles. Eur J Pharm Sci. 2005;25(4–5):357–67.
34. Kuntsche J, Westesen K, Drechsler M, Koch MJH, Bunjes H. Supercooled smectic nanoparticles: a potential novel carrier system for poorly water soluble drugs. Pharm Res. 2004;21(10):1834–43.
35. Hornig S, Bunjes H, Heinze T. Preparation and characterization of nanoparticles based on dextran–drug conjugates. J Colloid Int Sci. 2009;338:56–62.
36. Coates J. Interpretation of infrared spectra, A practical approach in: encyclopedia of analytical chemistry. In: Meyers RA, editor; 2000. p. 10815–10837.
37. Pawlak A, Mucha M. Thermogravimetric and FTIR studies of chitosan blends. Thermochim Acta. 2003;396:153–66.
38. Zheng H, Du YM, Yu JH, Huang RH, Zhang LN. Preparation and characterisation of chitosan / polyvinyl alcohol blend fibres. J Appl Polym Sci. 2001;80(13):2558–65.
39. Lambert JB, Shurvell HF, Lightner DA, Cooks RG. Organic structural spectroscopy. New Jersey: Prentice Hall Inc.; 1998.
40. Amato ME, Djedani F, Pappalardo GC, Perly B, Scarlata G. Molecular modeling of β-cyclodextrin complexes with nootropic drugs. J Pharmaceut Sci. 1992;81:1157–61.
41. Kumar DPS, Subrata C, Soumen R. Formulation and evaluation of solid lipid nanoparticles of A poorly water soluble model drug, ibuprofen. Int Res J Pharm. 2012;3(12):132–7.
42. Krupa A, Majda D, Jachowicz J, Mozgawa W. Solid-state interaction of ibuprofen and Neusilin US2. Thermochim Acta. 2010;509:12–7.
43. Manrique J, Martínez F. Solubility of ibuprofen in some ethanol + water cosolvent mixtures at several temperatures. Lat Am J Pharm. 2007;26(3):344–54.
44. Filippa MA, Gasull EI. Ibuprofen solubility in pure organic solvents and aqueous mixtures of cosolvents: interactions and thermodynamic parameters relating to the solvation process. Fluid Phase Equilib. 2013;354:185–90.
45. Perrie Y, Rades T. FFASTtrack pharmaceutics - drug delivery and targeting. 1st ed. London: Pharmaceutical Press; 2010.
46. Belmares M, Blanco M, Goddard WA, Ross RB, Caldwell G, Chou S, *et al.* Hildebrand and Hansen solubility parameters from molecular dynamics with applications to electronic nose polymer sensors. J Comput Chem. 2004;25(15):1814–26.
47. Fedors RF. A method for estimating both the solubility parameters and molar volumes of liquids. Polym Eng Sci. 1974;14(2):147–54.
48. Barton A. Handbook of solubility parameters and other cohesion parameters. 2nd ed. New York: CRC Press; 1991. p. 157–93.
49. Krug RR, Hunter WG, Grierger RA. Enthalpy-entropy compensation: separation of chemical from statistical effects. J Phys Chem. 1976;80(21):2341–51.
50. Mallick S, Pattnaik S, Swain K, De PK, Saha A, Ghoshal G. Formation of physically stable amorphous phase of ibuprofen by solid state milling with kaolin. Eur J Pharm Biopharm. 2008;68:346–51.
51. Desai SJ, Singh P, Simonelli AP, Higuchi WI. Investigation of factors influencing release of solid drug dispersed in inert matrices II. Quantification of procedures. J Pharm Sci. 1966;55:1224–9.